Interaction of Peroxynitric Acid with Solid H_2O-Ice

Zhuangjie Li, Randall R. Friedl, Steven 11. Moore, and Stanley l). Sander
Jet Propulsion laboratory, California Institute of Technology, Pasadena, California 91109

Abstract

The uptake of peroxynitric acid (PNA), HO_2NO_2 or HN04, on solid H_2O-ice at 193 K (-80 ^{0} C) was studied using a fast flow - mass spectrometric technique. An uptake coefficient of 0.15 ± 0.10 was measured, where the quoted uncertainty denotes two standard deviations. The uptake process did not result in the production of gas phase products. The composition of the condensed phase was investigated using programmed heating (3 K/rein) of the substrate coupled with mass spectrometric detection of desorbed species. Significant quantities of 1 INO_4 and I IN03 dcsorbcd from the substrates at temperatures above 225 K and 246 K, respectively. The desorbed HNO_3, which was less than 9% of the desorbed HN04 and remained unchanged upon incubation of the substrate, was likely due to impurities in the HN04 samples rather than reaction of HN04 on the substrate. The onset temperatures for HN04 desorption increased with increasing H_2O to HN04 ratios, indicating that HNO_4, like HNO_3, tends to be hydrated in the presence of water. These observations suggest possible mechanisms for removal of 11N04 or repartitioning of NO_y in the Earth's upper troposphere and stratosphere.

Introduction

The atmospheric NO_x and HO_x families are coupled together by two reactions resulting in acid formation [*Niki et al., 1977; Howard*, 1977, *Anderson et al., 1974]*, namely,

$$HO_2 + N02 + M \rightarrow HOON02 + M \quad (1)$$

$$OH + N02 + M \rightarrow HONO_2 + M \quad (2)$$

The important role of nitric acid, HNO_3, as a relatively stable reservoir of atmospheric NO_x has long been recognized from global gas-phase model calculations and field observations [*Hudson and Reed, 1979]*. Recent laboratory and field studies have also identified HNO_3 as a key species in denitrification of the wintertime polar stratosphere through gas/particle subsidence [*Molina et al.*, 1987, *Fahey et al.*, 1990, *Considine et al.*, 1992, *Kondo et al.*, 1994].

Peroxynitric acid, HN04, has received considerably less attention due to its relatively low atmospheric abundance. Although atmospheric production rates of HN04 are approximately equal to those of HN03 in the lower stratosphere and upper troposphere (e.g. at 20 km 1'(1 HNO_4)/P(I IN03) = k 1 /k2 x $[HO_2]/[OH] \approx 0.1 \times 7 = 0.7$) [*DeMore et al.*, 1994], ambient concentrations of HNO_4 are significant] y less than H N 03 due to relatively rapid photolysis of HNO_4 and reaction of I IN04 with 011.

$$HNO_4 + hv \rightarrow Products \quad (3)$$

$$OH + HNO_4 \rightarrow Products \quad (4)$$

Based upon existing kinetics data, the lower stratospheric lifetime of HNO_4 with respect to these processes ranges from approximately several days in the summer tropics to several weeks over the springtime pole *[Graham et al., 1977* and 1978]. Since both processes involving HNO_4 likely regenerate HO_2 and N02 in the atmosphere, the role of HNO_4 relative to HNO_3 is presumably that of a short- or medium- term nitrogen reservoir.

1 leterogeneous processing of stratospheric H N04 carries the potential to substantial] y alter the role of 11N04. in NO_y chemistry. Since HNO_4 can be viewed as an inorganic peracid, a mixed hydride of two acids, or as a peroxynitrite, it may participate in free radical

and/or ionic reactions; the latter type having been postulated to explain the heterogeneous reaction of HCl with $ClONO_2$, a reaction that is largely responsible for formation of active chlorine in the polar stratosphere [*Molina et* al., 1987]. In the case of HN04, heterogeneous chemical pathways of interest are those that result in a significant shift in the NO_y partitioning towards either more active NO_y species (i.e. NO, NO_2, or HONO) or the less active NO_y species such as HNO_3. Previous investigations have provided some evidence for the former pathway. In particular, Zhu et al. [1993] have obtained evidence for formation of HONO from the decomposition of HN04 on glass at 298 K. Logager and Schested [1993] have proposed that decomposition of PNA in solution is initiated by unimolecular decomposition to yield HONO.

The potential atmospheric impact of HN04 heterogeneous chemistry can be constrained by consideration of the collision rate (z) between HNO_4 and the background aerosol,

$$z = (c/4)A \qquad (I)$$

where c is the average HNO_4 velocity and A is the area density of stratospheric aerosol. At 20 km altitude, where a typical value of A is 6 x 10-9 $cm^2 cm^{-3}$ [*Turco et al., 1982; Deshler et al.*, 1992] and c is approximately 2 x 10^4 cm S-l, the collision rate is 3 x 10^{-5} S-l. Since the loss rate of HN04 is equal to the product of the collision rate and the fraction of collisions (γ) resulting in reaction, the value for γ must be greater than 0.03 for heterogeneous loss rates to bc competitive with photo] ysis and reaction with011.

In the present study we have obtained data on the interaction of HN04 with solid H_2O-ice and HCl-doped H_2O-ice. Experimental results were obtained using both a traditional, steady state flow tube technique and a fast switch variant of the flow tube technique. The latter technique was used to check for surface saturation by HNO_4. In this paper wc report results from both experimental approaches and derive surface probabilities for HN04 on solid H_2O-ice and HC1-doped H_2O-ice.

Experimental

The experimental apparatus (Figure 1) and its application to gas - solid interactions arc discussed in detail elsewhere [*Friedl et al.,* 1995]. In brief, the apparatus consisted of a conventional fast flow reactor that was modified for heterogeneous studies at low temperature and a mass spectrometer connected to the downstream end of the reactor. A 40-cm-long, 2.54 -cm-o.d. Pyrex tube served as the main reactor. PNA was admitted into the reactor through one of three ports, namely, a 120-cm long, 0.63-cm o.d. moveable injector that was heated with nitrogen gas at room temperature and coaxial with the reactor tube, or one of a set of entrance ports located 3-cm upstream and downstream of the cooled portion of the reactor. A 4-way valve connected to each of the latter set of ports by 3.2-mm diameter PTFE tubing allowed the PNA flow direction to be rapidly switched between the downstream and upstream ports. The time delay in PNA arrival at the detector caused by switching the 4-way valve was estimated to be less than 50 milliseconds, based on a sample flow velocity of -2,800 cm s^{-1} and a maximum traveling distance of 140 cm after alteration of the flow direction.

The reactor temperature was controlled by circulation of cooled methanol through an outer P yrex j acket and measured by a pair of thermocouples located at the downstream and upstream ends. For the current experiments temperat ures were maintained at 184-193 K with an overall measurement accuracy of ±1 K. The methanol circulator was equipped with a heater that served to either stabilize the temperature to within ± 0.5 K or warm up the reactor at a rate of about 3 K minute 1.

Ice films were prepared by bubbling helium carrier gas through a liquid water trap and passing the saturated gas flow into the reactor through the sliding injector. Film deposition was initiated with the injector tip at the downstream edge of the cold jacket and proceeded by withdrawal of the injector in 1 cm increments. The thickness of the ice film was controlled by varying the deposition time between each injector movement. 1 deposition times were varied between 10 seconds and 2 minutes, resulting in film thicknesses between 13 µm and 160 µm, respect ivel y. (Calculation of film thickness was accomplished by consideration of 'the

geometric surface area of the reactor wall (8 cm2 cm^{-1}), the amount of deposited water, and the bulk density of vapor-deposited water ice (i.e. *0.63* g cm^{-3} [*Keyser et. al.,* 1993]). The amount of ice was calculated from the water vapor pressure at 293 K, the mass flow rate of the helium-water mixture, and the total deposit time. Some of the deposited ice samples were collected in a [J-tube at 77 K and weighed on an analytical balance. It was found that the calculated amount of water agreed with that measured within 5%.

HNO_4 was synthesized by slowly adding ~1g NO_2BF_4 (Aldrich) into -5 ml of cold (≈0 °C) 90% 11202 [*Kenley et al.*, 1981]. The solution containing the I IN04 was transferred to a glass bubbler for usc in the experiments. The bubbler was maintained at 273 K and was connected to the flow reactor via 0.25 inch o.d. Teflon tubing. A cold trap (-258 K) was inserted bet ween the HNO_4 sample bubbler and the reactor in order to reduce the amount of H_2O_2 impurity in the gas flow. I IN04 sample flows were established by passage of helium through the bubbler.

The purities of several 1 HNO_4 samples were checked by filling a small absorption cell and subject i ng it to Fourier transform infrared analysis. Infrared spectra were taken by a Bomem DA3+.002 Fourier transform spectrometer equipped with a liquid nitrogen-cooled Cu:Ge detector. impurities in the HN04 solution were identified in the IR spectrum and ascribed to H_2O_2, HNO_3, NO_2, and H_2O. The relative amounts of the impurities varied between HN04 samples. However, greater than 10-fold reduction of HNO_3 and NO_2 impurities could be achieved by bubbling helium through the sample solution for -20 minutes prior to experimental use of the sample. The 258 K cold trap was found to reduce the amount of H_2O_2 by approximately a factor of 5, although H_2O_2 remained along with H_2O, the major impurities entering the reactor.

The Extranuclear electron impact mass spectrometer system employed in this study consisted of an ionizer operated at *25* eV, a quadruple mass filter, and a channeltron. Beam modulation was achieved with a *200-Hz* tuning fork type chopper placed i nside the second stage of the three-stage differentially pumped than ıber. Ion beam signals from the

channeltron were fed to a lock-in amplifier (Stanford Research Systems model 510), and stored on a personal computer following signal digitization with a computer-resident analog to digital converter (Analog Devices RTI/815).

HNO_4 was monitored at m/e ratios of 33, 46, and 30. Mass spectral intensities of I IN04 as well as the impurity species and/or reaction products H_2O_2, NO_2, HNO_3 and J I_2O arc given in '1'able 1. Although all of the HNO_4 mass peaks are subject to spectral interference from the other important species, in practice, the signal at m/e = 33 was essentially free from 11202 interference on account of the extremely low H_2O_2 sublimation pressure at 193 K. This fact was confirmed by checking for signal at the H_2O_2 parent peak at m/e = 34. The signals at m/c = 46 and n-de = 30 were slightly more problematic, however, 11N04 and N02 could be differentiated by their substantially different signal ratios (i.e. [m/e=46]/[m/e=30] = 7 for HN04 and 1.1 for N02) and contributions due to HN03 could be disccrncd by reference to the unique parent peak at m/c = 63. The mass spectra of HONO was not characterized for this experiment, however, we expect that its fragmentation pattern resembles that of N02 rather than 11 N04.

Approximate calibrations of the mass spectral signals were obtained for all of the species listed in Table 1. For the stable gases such as HNO_3, N02, and H_2O_2, dilute samples were prepared and absolute concentrations were obtained from measurements of cell pressures and gas flow rates. For HN04, concentrations were determined from the flow rate of helium carrier gas and the fraction of HN04 in the flow. The 1 IN04 partial pressure in the bubbler was derived from infrared absorbance of gaseous samples extracted from the bubbler using the HNO_4 cross sections reported by Molina and Molina [1 981] and Graham et al. [1 978].

For most investigations of HNO_4 uptake on substrates, partial pressures of gaseous 1 HNO_4 in the reactor were restricted to less than 0.1 mtorr. Based upon data from Kenley et al. [198 1] and May and Friedl[1993], wc estimate that these amounts arc significantly less than the equilibrium vapor pressure of HNO_4 at 193 K. Several measurements for 1 HNO_4

uptake on ice were made with PNA partial pressure greater than 0.1 mtorr to examine the effect of PNA concentration on the sticking process.

Results

Fast-Switch Transient Experiments

A qualitative appraisal of the interaction between 1 HNO_4 and solid H_2O-ice was accomplished by rapidly exposing the entire icc substrate to the gas flow and observing the transient signal behavior. Exposure of a surface to I IN04 was initiated by switching the gas flow from an entry port located near the mass spectrometer inlet and downstream of the substrate to one located upstream of the substrate. The additional transit distance of the flow was responsible for a rapid initial decrease in observed signal followed by rapid recovery. The transit time was approximately ***50*** ms as determined from a switched flow experiment through an uncoated, room temperature reactor.

Typical I HNO_4 temporal profiles arc shown in Figures 2 and 3 for cold-uncoated and -coated reactors, respectively. In the cold-uncoated reactor case signal recovery was characterized by two rates; a fast rate (1%/ms) similar to that observed in the room temperature reactor but prematurely ending at only 80% signal recovery, and a slow subsequent rate (< 0.25 %/min) extrapolating to signal recovery on timescales greater than one hour. Although the signal behavior clear] y indicates the occurrence of HNO_4 uptake on the reactor walls, no gas phase signals attributable to likely reaction products were dctectcd. Based on these observations alone, it is unclear whether the observed uptake phenomenology is attributable to HNO_4 condensation, where the inferred sublimation pressure would equal a value 0.8 times the initial HNO_4 vapor pressure (=0.1 mtorr), or to interaction of I IN04 with condcnscd impurities present in the HNO_4 such as H_2O and H_2O_2. Based on our measurements of the impurity levels in the I I N04 samples, the thi ckncsscs of films resulting from deposition of the impurities over the course of the observations were on the order of 0.1 μm. Amounts of deposited 1 HNO_4 were of the same order as the impurity deposits.

A dramatically enhanced uptake of I IN04 was observed in the ice-coated reactor case, providing strong evidence for the occurrence of a substantial interaction between the 1120-ice and HNO_4. Saturation of the surface, as indicated by signal recovery, occurred at a relatively slow rate of approximate] y 4%/min for the first 20 minutes, level ing off to a rate of less than 0.25%/min thereafter. The continuation of 1 IN04 uptake after 20 minutes is similar 10 the behavior observed in the uncoated case and, in light of profound uptake at early times, is most like] y attributed to additional H N04 uptake on fresh deposits of H_2O impurities contained in the HNO_4 flow.

The amount of HNO_4 deposited during the first 20 minutes is on the order of 1019 molecule, far exceeding monolayer coverage ($\theta > 1$) of the 20 cm long ice covered surface (θ was calculated assuming a momolayer of I IN 04 to bc approximatel y 5 x 1014 molecule cm^{-2} [*Hanson*, 1992], As in the uncoated case, an exhaustive mass spectra] search provided no evidence for production of gas phase species from the surface interaction. Possible alternative explanations for the large uptake include reactions to produce condensed phase species such as HNO_3, availability y of internal icc surface area, or formation of HNO_4 hydrates or solid 1 HNO_4/H_2O solutions. Additional information on these possibilities was obtained during the desorption experiments to be described in a later section of this report.

Moveable Injector Experiments

As revealed by the results of the fast switch flow technique, the H_2O-ice substrates adsorb significant quantities of HN04 but are eventually saturated with respect to further uptake. The slow rate of the saturation process allowed us to make precise measurements of the I IN04 uptake kinetics (i.e. sticking probability) using the commonly employed moveable injector technique. Kinetics data were obtained by passing HNO_4 through the moveable injector and admitting the flow into the reactor at various points along the ice substrate. in a similar manner to the ice deposition procedure, the experimental trials were started with the injector tip at the downstream end of the ice coated region. The injector position was changed

in 5 cm steps at approximately 1 minute intervals to allow for signal averaging and data collection.

The method used for retrieving sticking coefficients from the collected data is well known [*Howard*, 1979]. For a significant first-order wall loss in a steady-state tubular flow reactor, the loss rate can be written simply as,

$$d[HNO_4]/dt = \langle u \rangle d[HNO_4]/dz = -k[HNO_4] \quad (11)$$

where k is the first-order rate constant, t is the contact time between the reactor wall and the gas flow, and $[HNO_4]$ is the concentration of HN04 at time t, The contact time is calculated from the average carrier flow velocity, <u>, and the distance travelled by the flow after exit from the moveable injector. The rate constant can be determined from a regression of a plot of the logarithm of 1 IN04 signal vs. time.

Figure 4 represents a typical plot of the logarithm of PNA signal (m/e =46 and 33) vs. time. The observed logarithmic signal decays displayed good linearity over the time domain st udied and retrieved decay slopes were essentiall y identical for the m/e = 33 and m/e = 46 signal data. Data were corrected for radial and ice pore diffusion using the program developed by *Brown* [1978] and modified by *Keyser et al. [1991]*. The sticking coefficient, γ (i.e. the fraction of surface collisions resulting in removal of HNO_4), is calculated from

$$\gamma = 2r_o k_c/(\omega + r_o k_g) \quad (III)$$

where r_o is the radius of the reactor and ω the average molecular speed. We carried out a total of 23 runs on icc with the following range in parameters: film thicknesses between 13 and 160 μm, total reactor pressures between 0.5 and 1 torr, total flow rates between 500 and 1000 Seem , temperatures between 183 and 193 K, and initial HN04 partial pressures between 0.012 and 0.45 mtorr.

The results for each experimental trial are Ii steal in Table 2. Calculated sticking coefficients for 1 HNO_4 on icc arc independent of the experimental conditions related to ice thickness, temperature, and initial HNO_4 concentration. Combining all of the experimental

data yields an average value for the slicking coefficient of 0.1530.10, where the reported uncertainty is at the 2σ limit.

As a slight extension of this study, we briefly investigated the possibility of a heterogeneous reaction involving HNO_4 and HCl. We first doped I HCl (~4 x 10^{20} molecules) on the ice surface, and then introduced PNA to the ice surface with and without introducing I HCl in the gas phase. No change in the measured uptake coefficient relative to the HNO_4/H_2O-ice only case was observed, indicating the absence of a significant heterogeneous reaction between HNO_4 and 1 HCl at low temperature. In support of this conclusion we were unable to detect any new gas-phase chlorine-containillg species such as HOCl or Cl_2.

Product Studies

As stated previously, a methodical mass spectral search conducted in concert with I HNO_4 uptake trials revealed no evidence for new gas phase species. The lack of gaseous product formation associated with the rapid, kwgc-scale uptake of HNO_4 on H_2O-ice points to the likelihood of physi- or chemi - adsorption of the HNO_4.

$$HO_2NO_{2(g)} + H_2O_{(s)} \rightarrow HO_2NO_{2(l)} + H_2O_{(s)} \qquad (5a)$$

$$\rightarrow HO_2NO_2 \cdot (H_2O)_{n(s)} \qquad (5b)$$

Another possibility is reaction of the HN04 to produce condensed or solvated species. An example of the latter process is given by reaction 5b or Sc which involves HN03 production.

$$HO_2NO_{2(g)} + H_2O_{(s)} \rightarrow H1202(s) + HNO_{3(s)} \qquad (5c)$$

Based on gas phase thermodynamics data, however, reaction 5c is estimated to be endothermic by approximatel y 5 kcal mol^{-1} [*DeMore et al,* 1994]. Since the HNO_4 samples

used in the current experiments can be in fact prepared by the aqueous phase equivalent of the reverse of reaction 5c [*Kenley et al., 1981],* it is unlikely that significant quantities of HNO_3 can result from reaction 5c. 1 lowever wc recognize that the thermochemical equilibrium between HN04 and HNO_3 as established in the original synthetic HNO_4 sample, was greatly altered by the subsequent purification procedures employed and by the deposition of excess quantities of 1120 in forming the ice substrate. Consequentl y, some 11N03 production is to be expected following 1 HNO_4 uptake, although the conversion rate should be relatively slow at the lower temperatures. The thermod ynamic consequences of HNO_3 and HN04 solvation and/or hydration may also serve to favor HNO_3 formation.

in order to investigate the nature of the condensed phase species we conducted several programmed beatings of prepared substrates. Preparation of the substrates typically involved subjecting ice-coated and uncoated walls to 30 minutes of HNO_4 gas flow prior to the heating procedure. The substrates were heated for 30 minutes at a constant heating rate of approximately 3 K minute^{-1}.

The on] y species observed to desorb from the substrates were I HNO_4, HN03, 11202, and 1120, as deduced from their characteristic mass spect ral fragmentat ion patt ems. Temperature profiles for some of the relevant mass peaks arc shown in Figure 5. In the case of Figure 5a, flowing HNO_4 gas through the cold Pyrex surface lead to observation of a very thin, slightly opaque frozen solid layer on the surface, and during the heating process some transparent, presumabl y liquid, spots on the layer were observed. Resorption of I IN04 from "uncoated" glass reactor walls began at temperatures slightly above 193 K and peaked at 208 K. in sharp contrast, desorption of HNO_4 from ice-coated reactor walls (Figures 5b and 5c) occurred at significant y higher temperatures, starting at 210 K and reaching a maximum at 225 K; no transparent spots were observed during the warming of the solid. For the latter case, the desorption temperature was independent of the ice film thickness. Since both cases actually involved I IN04 and H_2O, albeit with vastly differing amounts of H20, the shift in

the desorption temperatures between the two cases signals a significant change in the nature of the interaction between I HNO_4 and the H_2O-ice surfaces.

HNO_3 and H_2O desorbed from ice-coated reactor walls (Figures 5d and 5c) at roughly the same temperature (~246 K). Only small quantities of nitric acid were observed; comparison of integrated signal profiles indicate that the amounts of 1 IN03 desorbed from the ice were less than 9% those of HN04. The likely origins of the observed HNO_3 were as impurities in the I IN04 samples. In order to verify this hypothesis we performed a temperature programmed desorption on two identically prepared 1 HNO_4/H_2O-ice substrates. One of the substrates was heated immediately following preparation while the other was allowed to stand for about 3 hours at 193 K. No increase in the amount of desorbed HNO_3 was observed (±20%) in the second sample relative to the first. Based on this result we conclude that no appreciable heterogeneous reaction occurs between HNO_4 and H_2O-ice which produces 1 HNO_3. An upper limit of <1% was placed on the amount of HN03 produced by reaction of 1 IN04 with 1120-ice over the time scale of the uptake.

Discussion

The results of the present study demonstrate that 1 HNO_4 is rapidly adsorbed on H_2O-icc surfaces at -190K. The measured uptake coefficient of 0.15 ± 0.10 is quite similar to that of the related acid HN03 [*Leu*, 1988; *Davy and Somorjai*, 1971; *Hanson, 1992]*. Like nitric acid, peroxynitric acid uptake on H_2O-ice results only in condensed phase species. However, whereas the formation of solid solutions and hydrates have been well characterized in the HNO_3 case, phase relationships have not been explored for the HNO_4/H_2O system. in the present study wc have probed only a small region of the phase equilibra. In particular, vapor phase conditions during HNO_4/H_2O deposition were nearly identical for the coated and uncoated reactor trials [i.e. $P(HNO_4) \approx P(H_2O) \approx$ 0.1 retort] and wc expect that the same 1 lN04-hydrate, albeit unidentified, was formed in both cases. Coexistence of this hydrate with

pure H_2O-ice was the likely result of the ice-coated reactor trials, and was also a possible outcome of the uncoated reactor trials.

The likel y formation of three phases (hydrate/ice/vapor) in the coated reactor (i.e. excess I 120) case constrains the system to onl y one degree of freedom. As a result, the vapor pressures of 1 IN04 and 1120 are fixed for any given temperature. Upon substrate warming the vapor pressures increase along the ice-hydrate solidus until the liquid/hydrate/ice eutectic point is reached. Further warming results in a phase change to the liquid/ice system. The absence of observable liquid formation in the coated reactor desorption trials, as would be evidenced by film transparency, indicates that the hydrate evaporation dominates over its melting process.

The observed ordering of evaporation and melting events in the coated reactor case can be related to the steady state (as opposed to static) nature of the experiments. Since the flow tube was subject to continuous vacuum pumping during the warming phase of the programmed resorption experiments, vapor phase species were removed from the reactor along with the carrier gas. Accordingly, the temperature dependent behaviors of observed gas phase species were governed both by the equilibrium vapor pressure over the substrates and the amounts of solid remaining in the flow tube. In a typical programmed resorption experiment, approximately 10^{19} molecules of 1 HNO_4 were deposited on the substrate. The removal time of the HNO_4 depended on the equilibrium pressure; it was 10 min for HNO_4 pressure of 0.1 mtorr and only 1 min for pressures reaching 1 mtorr. Based on the observations wc conclude that the eutectic point corresponds to HNO_4 pressures on the order of 0.1 mtorr and the amount of initially deposited HNO_4 is insufficient to allow for the occurrence of the liquid phase change. By analogy with the NA'I '/ice system and based on the lack of liquid formation upon heating the 1{N04-hydrate/icc systcm, wc estimate that the hydrate/icc/liquid eutectic temperature could bc located a few degrees higher than the temperature corresponding to the observed maximum 11N04 vapor concentration (225 K).

The same reasoning applies to the HNO_3 observed desorption behavior. Given the gas phase conditions established during film deposition we expected the impurity HNO_3 to form NAT on the ice surface. According to the HNO_3/I 120 phase diagram [*Hanson*, 1990], vapor pressures of 1 INO_3 in equilibrium with nitric acid trihydrate (NAT)/water ice range between 3 x 10-9 torr at 190 K to 2 x 10-5 torr at 230 K (eutectic temperature). On account of the relatively small equilibrium 1 INO_3 vapor pressure, it did not require a large amount of solid/liquid phase HNO_3 to maintain gas/solid equilibrium conditions during the substrate warming. The amount of impurity HNO_3 deposited on the substrate ($\approx 10^{18}$ molecules), as determined from the integrated desorption signal (Figure 5d), was sufficient to allow the system to nearly reach the eutectic point before all of the HNO_3-containing phases evaporated.

To further illustrate the behavior of 1 IN03 we performed an additional programmed desorption experiment on ice substrate (160 μm thick) doped with approximately 4 x 10^{19} molecules of HNO_3. The result of the trial is showed in Figure 6. The absence of HNO_4 in the trial allowed us to monitor HNO_3 with higher sensitivity using the NO_2^+ fragment rather than the parent peak. The observed desorption behavior clearly supports the hypothesized initial formation of a NAT/ice solid. In particular, two HNO_3 desorption peaks are apparent at 228 K and 246 K, corresponding to eutectic and melting temperatures for NAT/ice/liquid and ice/liquid systems, respectively. Based on this information we conclude that an upper limit of-20% of the 228 K peak observed in the PNA experiments could be due to HNO_3.

Vapor pressures of HN04 in the uncoated reactor case were significantly higher, for a given temperature, than those in the coated reactor. Moreover, the film evaporated at a significantly lower temperature (208 K) than the predominately ice containing film. These observations suggest that the 11 NO_4-containing film deposited on the uncoated reactor corresponds to a pure hydrate. By analogy with HNO_3 the equilibrium HNO_4 vapor pressure above the hydrate is presumably greater than that above a hydrate/ice mixture. As an example

of this phenomena, Kochler et al. [1992.] observed the evaporation of HNO_3 from pure NAT at a temperature 10 K below the ice/NAT/liquid eutecti c temperature observed by us.

The 11N04-hydrate properties deduced from the above discussion carry important implications for denitrification of atmospheric air parcels. Although, typical ambient HN04 concentrations ($\leq$ 10-8 torr) arc far less than required to create pure 1 I NO_4-hydrates in the atmosphere, the uptake of 11N04 on existing polar stratospheric clouds or upper tropospheric cirrus clouds to form hydrate/water-icc mixtures is fast enough to compete with other photochemical HN04 loss processes. Sequestered I IN04 may then be removed, along with NAT, by large scale subsidence or deep downward convection. Further investigations of the HNO_4/H_2O phase equilibria arc required, however, to quantify these possibilities.

Acknowledgement

The research described in this paper was carried out at Jet Propulsion Laboratory, California Institute of Technology, under contract with the National Aeronautics and Space Administration. Wc thank R. Zhang and M-T Leu for helpful discussion on our results, and R.D. May for facility assistance in preparing HN04.

REFERENCES

Anderson, J. G., J.J. Margitan, and F. Kaufman, Gas phase recombination of OH with NO and N02, *J. Chem. Phys.*, *60,3310,* 1974.

Drown, R.] . . . Tubular Flow Reactors with First-Order Kinetics, *J. Res. Natl. Bur. S/and., 83, 1, 1978.*

Considine, D.B., A.R. Douglass, and R.S. Stolarski, Heterogeneous conversion of $N2_{0_5}$ to HNO_3 on background stratospheric aerosols: comparisons of model results with data, *Geophys. Res. Letts.*, 1 9,397, 1 992.

Davy, J. G., and G.A. Somorjai, Studies of the vaporation Mechanism of Ice Single Crystals, *J. Chem. Phys. , 55,3624, 1971.*

DeMore, W.B., S.P. Sander, D.M. Golden, R.F. Hampson, M.J. Kurylo, C.J. Howard, A.R. Ravishankara, C. E. Kolb, and M.J. Molina, *JPL Publication 94-26,* Jet Propulsion Laboratory, Pasadena, CA, December 15, 1994.

Deshler, T., D.J. Hofmann, B.J. Johson, and W.R. Rozier, Balloonborne Measurements of the Pinatubo Aerosol Size Distribution and Volatility at Laramie, Wyoming During the Summer of 1991, *Geophys. res. Letts., 19,* 1991992.

Fahey, D. W., K.K. Kelly, S.R. Kawa, A.F. Tuck, M. Loewenstein, K.R. Chan, and L.E. Heidt, Observations of denitrification and dehydration in the winter polar stratospheres, *NATURE,* 344,321, 1990.

Fried], R.R., S.B. Moore, and S.P. Sander, *J. Geophys. Res.*, in preparation.

Graham, R. A., A.M. Winer, and J.N. Pitts, Jr., Temperature Dependence of the Unimolecular Decomposition of Per-nitric Acid and its Atmospheric Implications, *Chem. Phys. Lett., 51, 215, 1977.*

Graham, R. A., A.M. Winer, and J.N. Pitts, Jr., Pressure and temperature Dependence of the Unimolecular Decomposition of HO_2NO_2, *J. Chem. Phys.*, 68,4505, 1978.

Graham, R. A., A.M. Winer, and J.N. Pitts, Jr., Ultraviolet infrared absorption cross sections of gas-phase HO_2NO_2, *Geophys. Res. Lett.*, 5, 909, 197X.

1 Ianson, D. R., The Uptake of HNO_3 Onto Icc, NAT, and Frozen Sulfuric Acid, *Geophys. Res. Letts.*, 19,2063, 1992.

I Ianson, D. R., The Vapor Pressure of Supercooled HNO_3/H_2O Solutions, *Geophys. Res. Letts.*, 17,421, 1990.

I Ioward, C. J., Kinetics of the Reaction of HO_2 with $N0_2$, *J. Phys. Chem.*, 67, 1977.

Ioward, C. J., Kinetic Measurements Using Flow Tubes, *J. Phys. Chem.*, 83, 3, 1979.

Hudson, R. D., and E.I. Reed, The Stratosphere: Present and Future, *NASA Reference Publication 1049,* 1979.

Kenley, R. A., P.L. Trevpr, and B. Y. Ian, Preparation and thermal Decomposition of Pernitric Acid (1 $HOONO_2$) in Aqueous Media, *J. Am. Chem. SIX., 103,2203,* 1981.

Kcyscr, L.F., S.B. Moore, and M. T. Leu, Surface Reaction and Pore Diffusion In Flow-Tube Reactor, *.1. Phys. Chem.*, 95,5496, 1991.

Keyser, 1..17., M.-'l'. Leu, Surface Areas and Porosities of Ice Used to Simulate Stratospheric Clouds, J. *Colloid Interface Sci.*, 155, 137, 1993.

Kondo, Y., W.A. Matthews, S. Solomon, M. Moike, M. Hayashi, K. Yamazaki, H. Nakajima, and K. Tsukui, Ground-based measurements of column amounts of N02 over S yowa Station, Antarctica, *J. Geophys. Res.*, 99, 14535, 1994.

Leu, M.-T., laboratory Studies of Sticking Coefficients and 1 leterogeneous Reactions important in the Antarctic Stratosphere, *Geophys. Res. Lett., 15,* 17, 1988.

Logager, '1'., and K. Schested, Formation and Decay of Peroxynitric Acid: A pulse Radiolysis Study, *J. Phys. Chem. ,97,* 10047,1993.

May, R. D., and R.R. Friedl, integrated Band Intensities of 1 IO_2NO_2 at 220 K, J. *Quant. Spectrosc. Radiat. Transfer, 50,257,* 1993.

Molina, L. T., and M.J. Molina, UV Absorption Cross Sections of $H0_2N0_2$ Vapor, J. *Photochem., 15,97,* 1981.

Molina, M. J., T-L "l'so, L. T. `.Molina, and F. C-Y Wang, Antarctic Stratospheric Chemistry of Chlorine Nitrate, Hydrogen Chloride, and Ice: Release of Active Chlorine, *Science*, 238, 1253, 1987.

Niki, 11., P.D. Maker, C.M. Savage, and L.P. Breitenback, Fourier Transform I R Spectroscopic Observation of Pernitric Acid Formed via HOO + $N0_2 \rightarrow$ $HOON0_2$, *Chem. Phys. Lett. ,45,564,* 1977.

Truco, R.] '., R.C. Whitten, and O.B. Toon, Stratospheric Aerosols: Observation and Theory, Rev. *Geophys. Space Phys. ,20,233,* 1982.

Zhu, '1'., G. Yarwood, J. Chen, and H. Niki, Evidence for the 1 leterogeneous Formation of Nitrous Acid From Peroxynitric Acid in Environmental Chamber, *Environ. Sci. Technol.*, 2.7, 982, 1993.

'l'able 1. Mass Spectral Intensities* for Pernitric Acid (PNA), $N0_2$, H_2O_2, HNO_3, and H_2O.

	Ion					
	NO^+	HO_2^+	$H_2O_2^+$	HNO_3^+	NO_2^+	H_2O^+
Ill/c	30	33	34	63	46	18
I'NA	25	6			180	
NO_2	49				55	
H_2O_2		2	58			
HNO_3	9			3	93	
H_2O						10

* Values arc in mV/mtorr (except for the first row).

Table 2. Sticking probability for pernitric acid on ice surfaces.

h* (pm)	P_{total} (torr)	F_{total} (Seem)	Temp. (K)	[PNA] (mtorr)	$k_{obs.}$ (s^{-1})	k_g (s^{-1})	γ
13.5	0.92	997	192	0.038	364	1678	0.17
13.4	0.91	957	189	0.068	288	751	0.081
13.6	0.93	985	187	0.45	332	1363	0.14
13.9	0.50	530	193	0.063	349	580	0.063
13.7	0.50	533	193	0.060	436	881	0.090
13.5	0.50	536	193	0.33	510	1264	0.13
13.6	0.50	527	193	0.024	458	975	0.10
13.5	0.50	524	193	0.031	577	1824	0.19
13.5	0.50	523	189	0.056	566	1700	0.17
13.5	0.50	525	191	0.082	554	1598	0.16
81.5	0.95	1006	193	0.012	298	830	0.090
80.8	0.50	514	193	0.048	397	599	0.070
78.4	0.51	519	185	0.11	509	1502	0.16
79.7	0.51	520	189	0.044	524	1530	0.16
81.0	0.51	521	184	0.036	503	1474	0.16
81.4	0.51	524	186	0.033	499	1386	0.15
80.2	0.51	520	183	0.086	532	1824	0.19
159.3	0.51	521	191	0.033	596	2318	0.23
160.0	0.51	522	191	0.11	62>2	2828	0.27
160.2	0.51	527	190	0.055	600	2353	0.23
160.0	0.51	524	192	0.037	527	1496	0.16
160.0	0.51	527	189	0.041	522	1501	0.16
159.3	0.51	523	187	0.029	532	1667	0.17

* ICC thickness was calculated using the measured geometric area and weight of the deposited water with a value of 0.63 g cm^{-3} for bulk density of val)or-deposited water ice.

Figure Captions

Figure 1. Experimental setup for studying reaction of PNA with water at low temperature.

Figure 2. PNA signal as function of time when flowing PNA through Pyrex reactor surface at 190 K. The initial concentration of PNA was 1.5×10^{-5} torr.

Figure 3. PNA signal as function of time when flowing PNA through ice surface at 190 K. The thickness and the length of the ice film was 13.4 μm and 20 cm, and the initial concentration of PNA was 1.2×10^{-5} torr.

Figure 4. Typical PNA decay on ice surface (160 pm thick) at 189 K. The experimental conditions for the plot were: $P_{total} = 0.51$ torr, $P_{PNA} = 4.1 \times 10^{-5}$ torr, $v_{flow} = 1{,}800$ cm s^{-1}.

Figure 5. The signal intensity of different species as function of temperature after -10^{19} PNA molecules were adsorbed on the ice surface. About one gram ice was used to make the ice film with thickness of about 160 μm. The heating rate for the desorption of product mixture was ~3 K minute-1.

Figure 6. The nitric acid signal intensity as function of temperature. The nitric acid was introduced on ice surface by passing the nitric acid vapor at 195 K through the reactor coated with ice film (160 μm thick). 'l'he heating rate was ~3 K $minut^{-1}$.

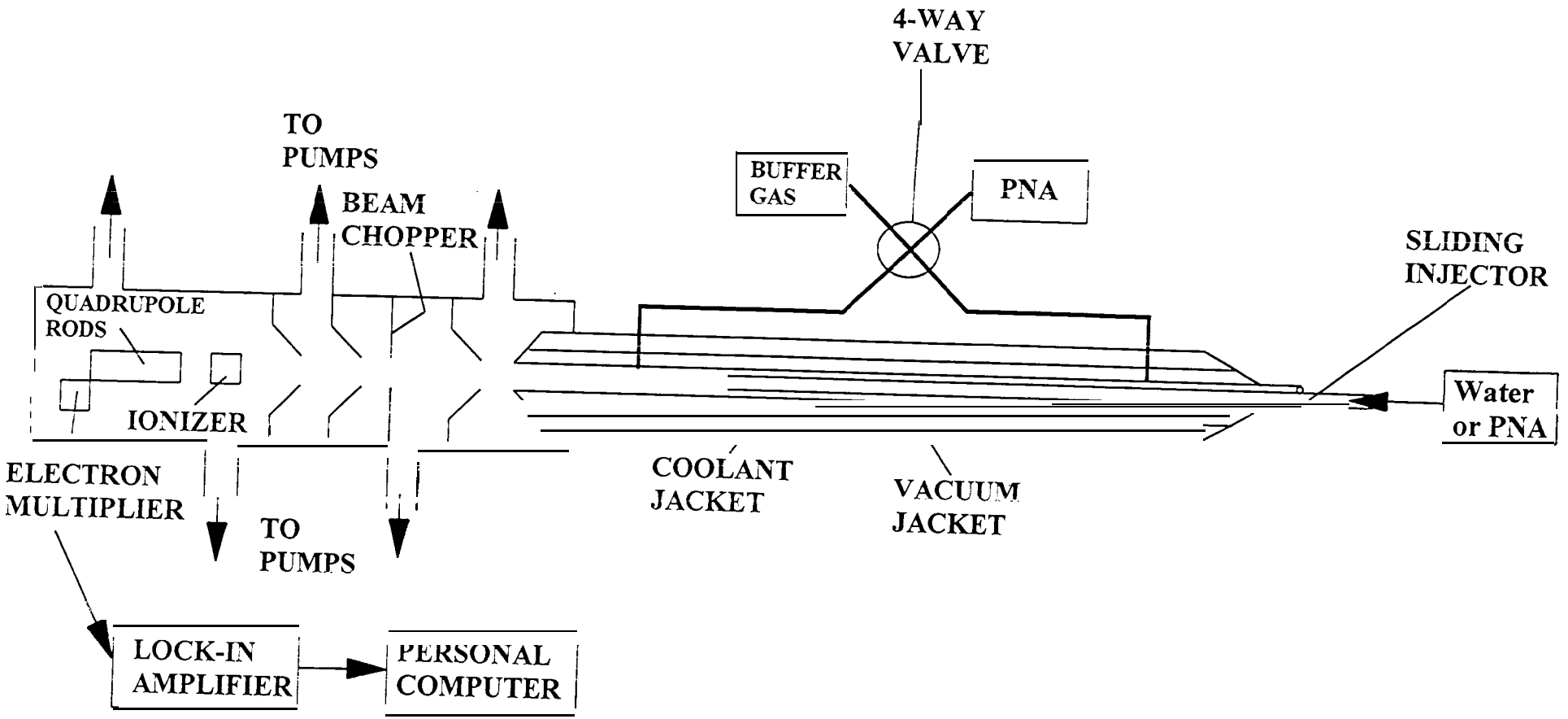
4-WAY
VALVE
TO
PUMPS
BUFFER
GAS
PNA
BEAM
CHOPPER
SLIDING
INJECTOR
QUADRUPOLE
RODS
IONIZER
Water
or PNA
ELECTRON
MULTIPLIER
TO
PUMPS
COOLANT
JACKET
VACUUM
JACKET
LOCK-IN
AMPLIFIER
PERSONAL
COMPUTER

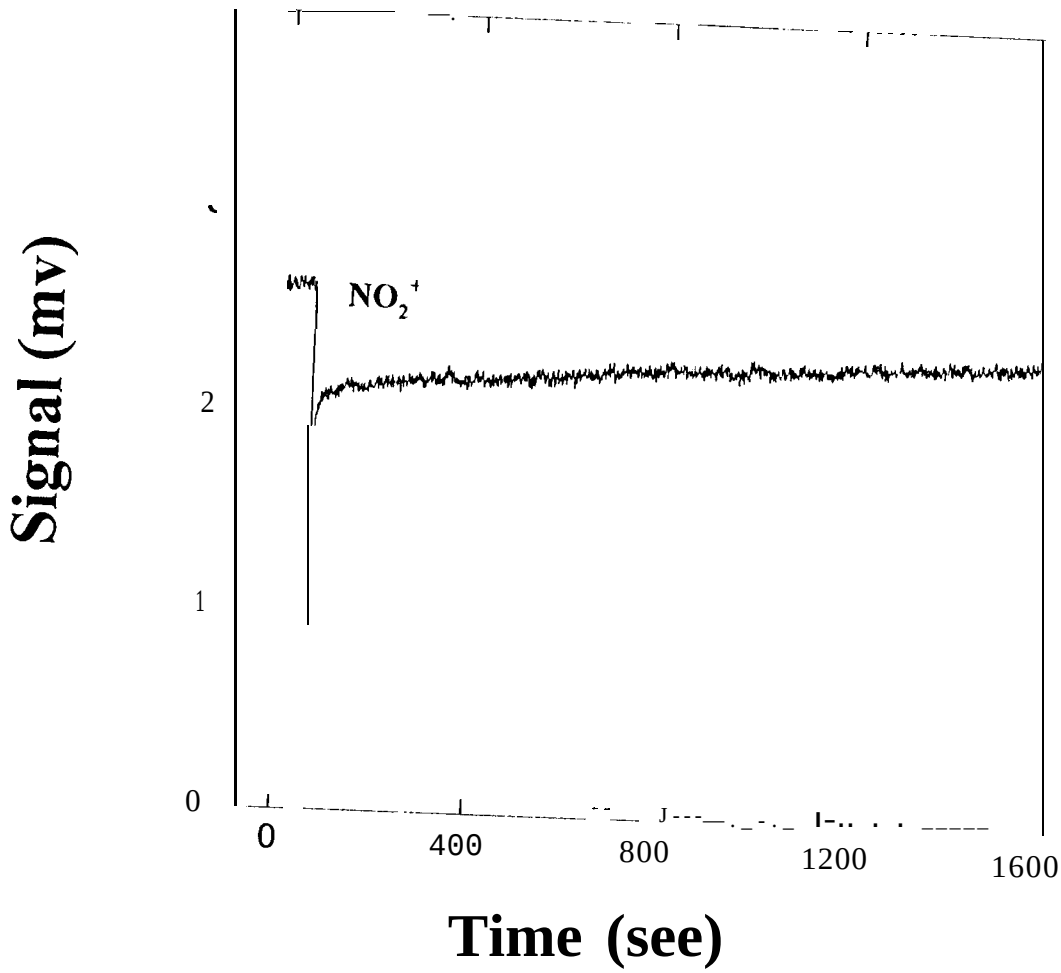
Signal (mv)
NO_2^+
2
1
0
0
400
800
1200
1600
Time (see)

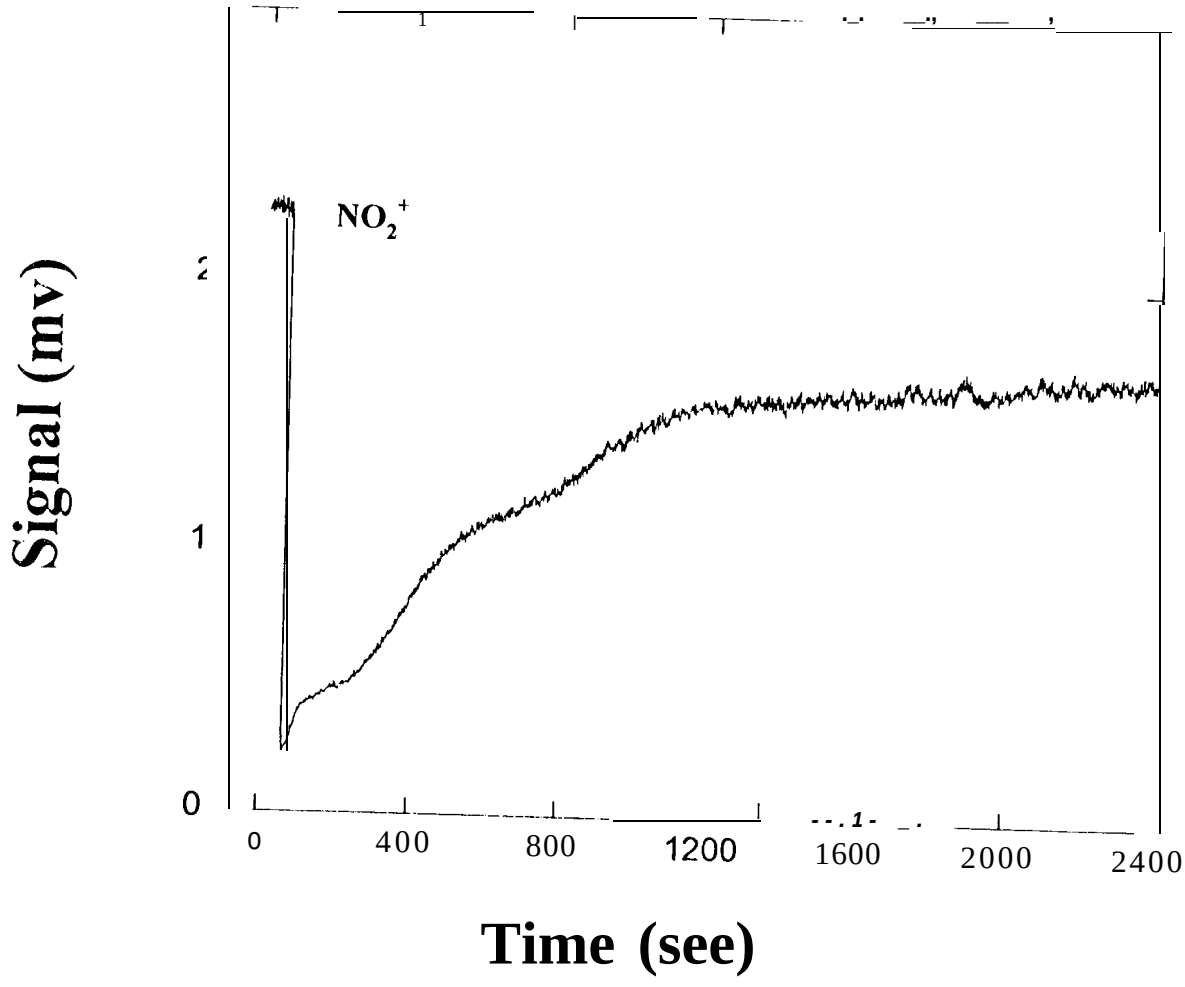
Signal (mv)
NO_2^+
2
1
0
0
400
800
1200
1600
2000
2400
Time (see)

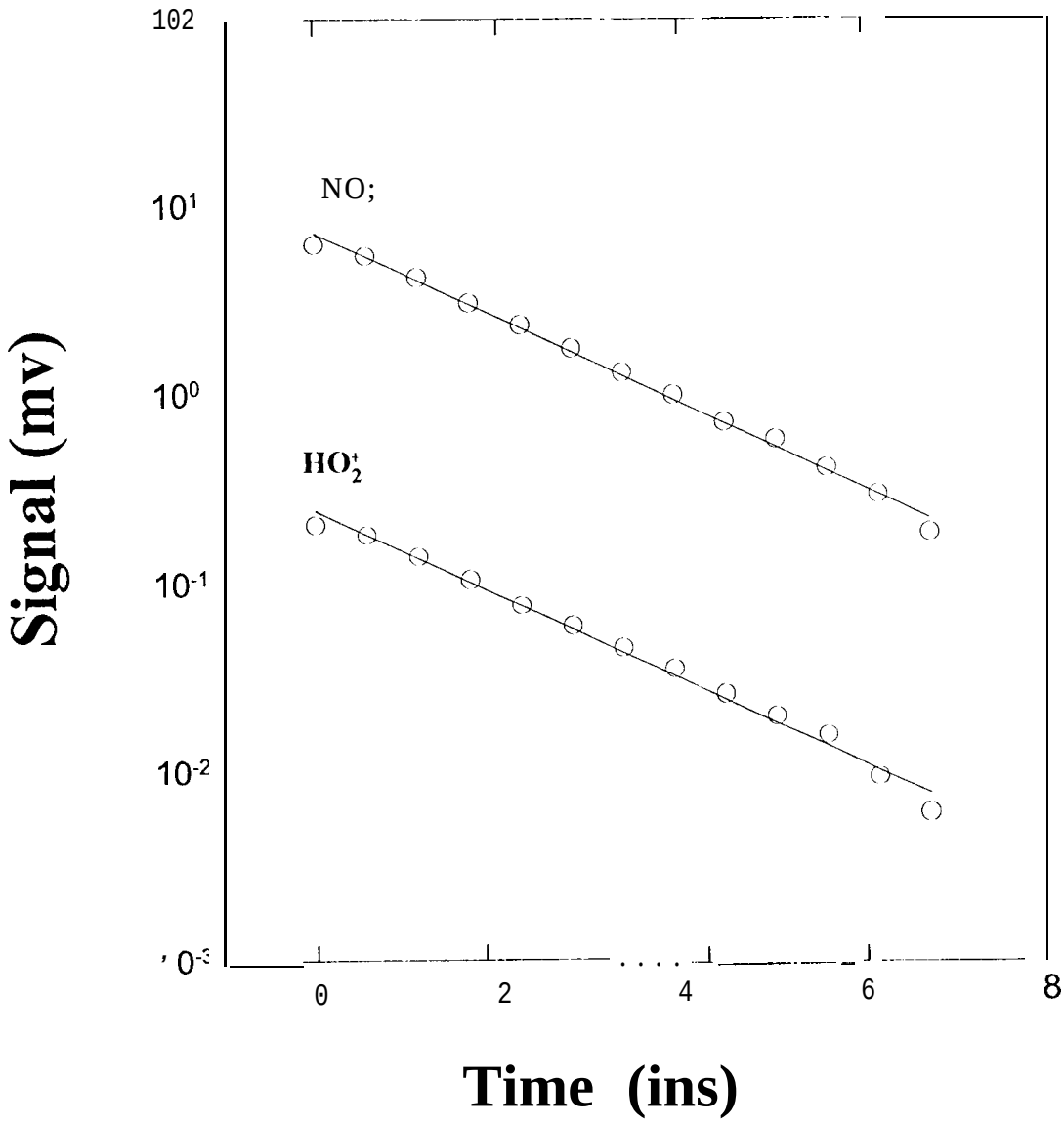
Signal (mv)
102
10^1
10^0
10^{-1}
10^{-2}
10^{-3}
NO;
HO_2^+
0
2
4
6
8
Time (ins)

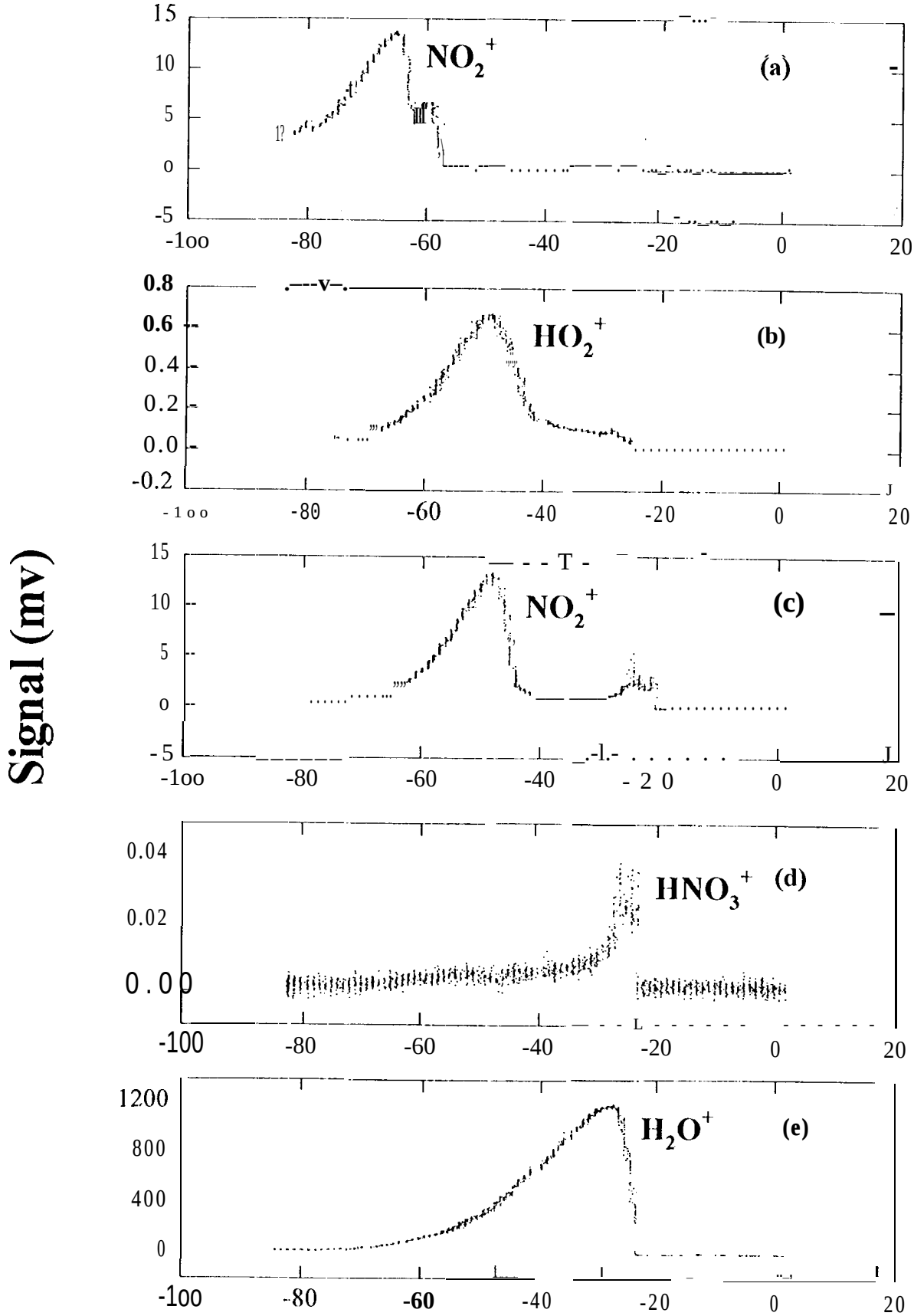
Signal (mv)
15
10
5
0
-5
NO_2^+
(a)
-1oo
-80
-60
-40
-20
0
20
0.8
0.6
0.4
0.2
0.0
-0.2
HO_2^+
(b)
-1oo
-80
-60
-40
-20
0
20
15
10
5
0
-5
NO_2^+
(c)
-1oo
-80
-60
-40
-20
0
20
0.04
0.02
0.00
HNO_3^+
(d)
-100
-80
-60
-40
-20
0
20
1200
800
400
0
H_2O^+
(e)
-100
-80
-60
-40
-20
0
20
Temperature (“C)

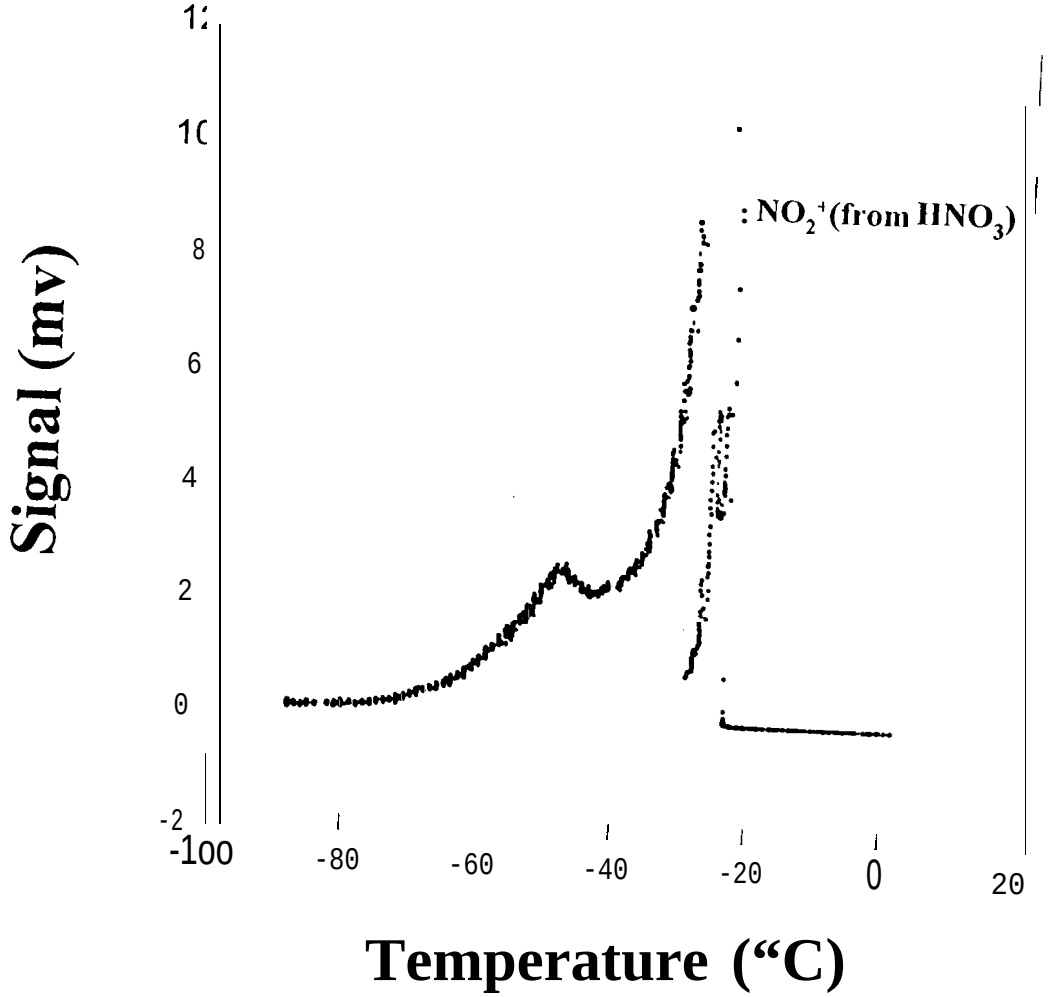
Signal (mv)
12
10
8
6
4
2
0
-2
-100
-80
-60
-40
-20
0
20
: NO_2^+(from HNO_3)
Temperature (“C)